Photolysis at 266 nm of argon matrix isolated ozone monomer

M. Bahou, L. Schriver-Mazzuoli, and A. Schriver

Citation: The Journal of Chemical Physics **110**, 8636 (1999); doi: 10.1063/1.478771
View online: http://dx.doi.org/10.1063/1.478771
View Table of Contents: http://scitation.aip.org/content/aip/journal/jcp/110/17?ver=pdfcov
Published by the AIP Publishing

Photolysis at 266 nm of argon matrix isolated ozone monomer

M. Bahou, L. Schriver-Mazzuoli,[a] and A. Schriver
Laboratoire de Physique Moléculaire et Applications,[b] Laboratoire propre du CNRS, Université Pierre et Marie Curie, Tour 13, case 76, 4 Place Jussieu, 75252 Paris Cedex 05, France

(Received 21 July 1998; accepted 27 January 1999)

The photodissociation of ozone trapped at high dilution in solid argon has been reinvestigated at different temperatures and various photon flux, combining irradiation at 266 nm and infrared spectroscopy. In argon, recombination of $O+O_2$ is a major pathway and the weak decrease of ozone is due to cage exit of oxygen atoms which is dependent of the temperature and of the initial photon flux. Kinetic curves are well fitted by a double exponential expression and a model based upon two different cage exit pathways is proposed. © *1999 American Institute of Physics.* [S0021-9606(99)01316-1]

INTRODUCTION

Photochemical reactions in a low temperature solid environment are of current interest in a variety of applications, and the technique of matrix isolation spectroscopy has been used for numerous studies of the photodissociation of small molecules[1–6] and of chemical reactions between atoms, ions, and radicals with stable molecules.[7–13]

UV photolysis of ozone in matrices is a good source of excited atomic oxygen and this technique has been extensively used to investigate reactions of atomic oxygen with various species in the solid state.[14–19] However diffusion and quenching of the $O(^1D)$ oxygen atom under matrix isolation conditions can play an important role and the knowledge of the photodissociation process of ozone is needed. The first UV photochemical studies of ozone in argon and nitrogen matrices have been reported by Benderskii and Wight[20,21] and later new information in the nitrogen matrix were given.[22]

In argon, from Ref. 20 interpretation of the photochemical kinetics was not entirely clear, due to limited spectral resolution or sensitivity and a complication was introduced by the presence of ozone clusters. Two steps were suggested involving first a photolysis process (fast) due to reactions in small clusters, then a second step (straight line in the kinetic plots) due to the dissociation of monomers.

In the present work, the photodissociation of ozone in argon was reinvestigated at 266 nm for samples with low concentrations of ozone in which ozone clusters are expected to be absent, which should simplify the analysis. The present study brings additional and more detailed information about the photodissociation dynamics of ozone from extensive studies of the ozone photodissociation at different photon flux and at different temperatures. The results show that the cage exit of oxygen atoms (which prevents ozone recombination from oxygen atom and O_2 molecule pairs) depends on both temperature and irradiation power. From the fit of observed kinetic curves by a double exponential expression, a mechanism is proposed.

EXPERIMENT

The cryogenic system used in the present studies consisted in a rotatable closed cycle refrigerator (Air Product 202 A) with KBr optical windows for performing IR reflection measurements and one quartz window for ultraviolet photolysis. Mixtures of gaseous reagents were deposited at 20 K onto a gold plated mirror at a rate of 10^{-2} mol/h. A temperature controller (Silicon diode 9600-1) was used to maintain the chosen temperature to within ± 0.1 K. Ozone was prepared from natural oxygen (Air Liquide N50) and $^{16}O_2/^{18}O_2$ mixtures (Eurisotop CEA) contained in a glass vacuum finger excited by a Tesla coil discharge with trapping of ozone at liquid nitrogen temperature. Residual oxygen was removed by freeze–pump–thaw cycles with liquid nitrogen. Argon (Air Liquide N56) carrier gas was used without further purification and several argon/ozone mixtures were prepared and deposited. The spectra were recorded with a FTIR Bruker IFS 113 v spectrometer in the reflection mode at a resolution of 0.1 cm^{-1}. We did unfortunately not get rid of impurities such as CO_2 and SiF_4 during the preparation of ozone. Weak absorption bands due to SiF_4 were measured at 1027.5 and 1023.1 cm^{-1}. Ozone photodissociation was carried out at 266 nm using the fourth harmonic of a Nd-YAG laser (YG 781 C-20 from Quantel) which operates at 20 Hz with 4 ns pulse duration. The light intensity was spatially homogenized with a divergent lens placed in front of the cryostat UV window. The fluence inside the cryostat was estimated from the power measured with a detector PSV 3102 Gentec S/N 61592 with a section of 1.76 cm^2 which was placed after the lens and a CaF_2 window simulating the entrance window of the cryostat.

At 266 nm, the primary process of ozone dissociation is namely the production of an oxygen atom in the first excited state (85%) (see Refs. 23, 24, and references therein). As in Ref. 22, results were first analyzed assuming that the photochemical decomposition of ozone was a first order process,

[a]Author to whom correspondence should be addressed. Also at Université Paris XIII.
[b]Laboratoire Associé aux Universités P. et M. Curie.

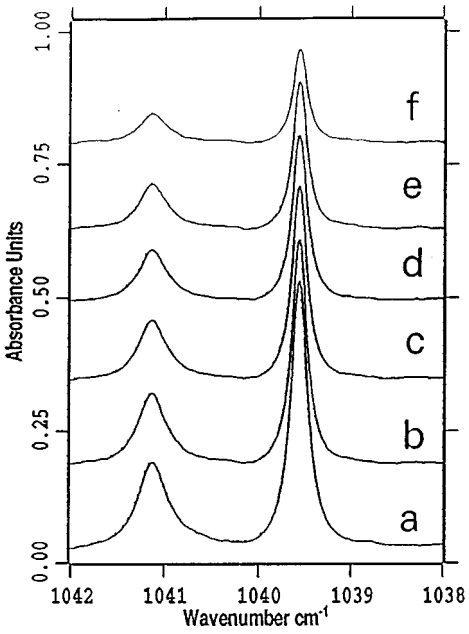

FIG. 1. FTIR spectra (resolution 0.04 cm^{-1}) recorded at 11 K in the v_3 ozone absorption region of an O_3/Ar mixture (O_3/Ar= 1/4000) after photolysis with the 266 nm laser line (photon flux, 3.8×10^{16} photons $cm^{-2}\,s^{-1}$). Irradiation times (a) 0 min; (b) 10 min; (c) 20 min; (d) 30 min; (e) 50 min; (f) 100 min.

$$-\frac{d[O_3]}{dt}=k(\lambda)[O_3]. \tag{1}$$

The photokinetic rate constant $k(\lambda)$ depends on the photodissociation cross section $\sigma(\lambda)$ in cm^2/molecule (base e) of ozone at $\lambda=266$ nm, the quantum yield $\varphi(\lambda)$, and of the photon flux $F(\lambda)$ in photons $cm^{-2}\,s^{-1}$,

$$k(\lambda)=\sigma(\lambda)\varphi(\lambda)F(\lambda). \tag{2}$$

Assuming an optically thin sample, the ozone concentration is proportional to the integrated absorption intensity of the each vibrational modes and for each set of experiments the quantity $f(t)=\ln(A^0_{O_3}/A^t_{O_3})=k(\lambda)t$ was plotted vs the total operating laser time ($A^t_{O_3}$ and $A^0_{O_3}$ are the ozone absorbances at time t and $t=0$, respectively).

RESULTS

In an argon matrix the three modes of normal ozone appear as doublets measured at 1105.1–1105.2 cm^{-1} (v_1), 703.6–704.3 cm^{-1} (v_2), and 1039.7–1041.2 cm^{-1} (v_3).[24] The lower components (the most intense ones) have been assigned to ozone in pairs of interacting sites, whereas the higher components (temperature sensitive) characterize ozone in a single site.[25] The v_3 absorption was chosen for monitoring ozone photodissociation because it is the strongest infrared band of ozone with the following intensities: $v_1/v_2/v_3=0.54/7.7/100$. Measurements were limited to an optical density less than 0.8. At the resolution used (0.1 or 0.04 cm^{-1}) and at low ozone concentration (O_3/Ar$\leqslant 2.5\times10^{-4}$) the two v_3 components of ozone are well resolved and have each another a full-width at half-maximum (FWHM) of 0.25 cm^{-1} (lower component) and 0.4 cm^{-1} (higher component), respectively. This band shape is different from the band shape observed in Ref. 20, where the v_3 components at 10^{-4} mol fraction are overlapped with a FWHM of 0.8 cm^{-1}. The quantity $\ln(A^0_{O_3}/A^t_{O_3})$ was measured from the lower wave number component except in some experiments where the decay of ozone trapped into the two sites was compared.

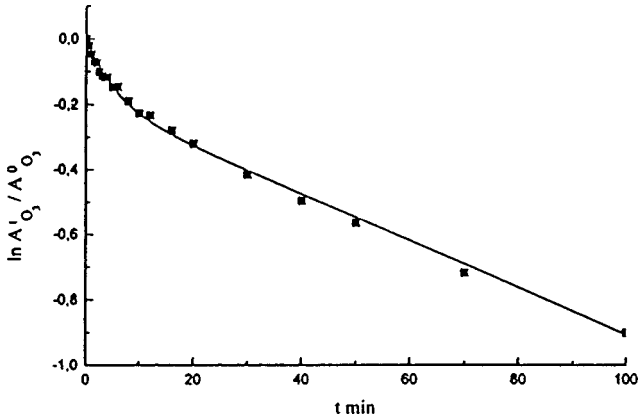

FIG. 2. Kinetic curve at 11 K and 266 nm for ozone photodissociation of an O_3/Ar= 1/4000 mixture. Photon flux, 3.8×10^{16} photons $cm^{-2}\,s^{-1}$.

Figure 1 shows typical spectra recorded at 11 K of the relatively slow intensity decrease of the v_3 ozone band as a function of the irradiation time ($F=0.38\times10^{17}$ photons $cm^2\,s^{-1}$). A very weak band at 1033 cm^{-1} appears also under irradiation, reaches a stationary state then decreases at a longer time. It was not represented in the figure because of its weak intensity (optical density of 0.006). It can be assigned from Ref. 26 to the $O_3\cdots O$ complex giving evidence of an oxygen atom exit as discussed later.

In Fig. 2 the kinetic curve at 11 K for the photolysis at 266 nm ($F=0.38\times10^{17}$ photons $cm^2\,s^{-1}$) of a diluted sample of ozone (O_3/Ar= 1/4000) is represented by plotting the quantity $\ln(A^t_{O_3}/A^0_{O_3})=\ln([O_3]^t/[O_3]^0)$ vs irradiation time. Data clearly indicate that the kinetics do not obey a first order process as implied by Eq. (1). The kinetic curve at 10

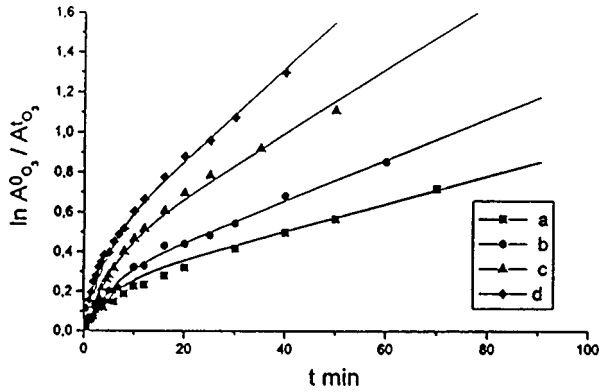

FIG. 3. Kinetic curves for ozone photodissociation at different initial photons flux (photons $cm^{-2}\,s^{-1}$); (a) 3.2×10^{16}; (b) 6.4×10^{16}; (c) 11.4×10^{16}; (d) 15.2×10^{16}; (O_3/Ar= 1/4000). Sample temperature during photolysis is 11 K. ■, ●, △, ◆ are the experimental data and the solid line is a fit of Eq. (3) to the data. The fitting parameters are summarized in Table I.

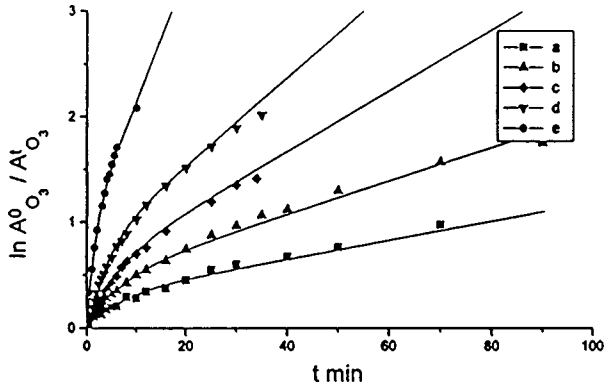

FIG. 4. Kinetic curves for ozone at different temperatures (a) 11 K, (b) 16 K, (c) 18.5 K, (d) 21 K, (e) 26 K; (O_3/Ar= 1/4000); photon flux, 3.8 $\times 10^{16}$ photons $cm^{-2}\,s^{-1}$. ■, △, ◆, *V*, ● are the experimental data and the solid line is a fit of Eq. (3) to the data. The fitting parameters are summarized in Table I.

K exhibits two distinct phases characterized by two different slopes with apparent rate constants of $0.92\times10^{-3}\,s^{-1}$ at $t=0$ and of $1.5\times10^{-4}\,s^{-1}$ at longer times with 60% of initial ozone remaining after 30 min of irradiation. Thus in spite of the absence of ozone dimers in our experiments, the kinetic curve for the disappearance of ozone is qualitatively similar to that reported in Ref. 20 and the first photolysis step (fast) is not due to a reaction in small clusters as proposed by Benderskii and Wight.

Figure 3 displays kinetic curves of the ozone photolysis at 11 K for different photon flux (from 0.3×10^{17} to 1.8×10^{17} photon $cm^{-2}\,s^{-1}$) and Fig. 4 shows the effect of temperature upon the kinetic curves for a photon flux of 0.38×10^{17} photon $cm^{-2}\,s^{-1}$. While the general shape of the curves remains essentially unchanged an important observation can be made; the two parts of the kinetic curves appear photon flux and temperature dependent. At 11 K (Fig. 3) for a high photon flux, the curve tends to be linear with one single slope. The same behavior occurs for a high temperature and low photon flux. Due to estimation of the irradiation photon fluence the errors involved in the experimental measurements of a_1 and a_2 were estimated to be 20%. Tables I and II summarize for all the different experimental conditions the slope of the tangent to the kinetic curve at $t=0(a_1)$ and that of the second linear part of the curve (a_2). In all experiments, no significant change in the relative yield of the $O_3\cdots O$ complex with regards to the ozone monomer was observed.

The experimental curves which reveal two different contributions, were well fitted by a double exponential expression of the type

$$\ln\frac{[O_3]^0}{[O_3]^t}=\ln[\alpha e^{\lambda_1 t}+(1-\alpha)e^{\lambda_2 t}]. \tag{3}$$

Values of α, λ_1, and λ_2 are reported in Tables I and II. As can be seen, the derived λ_2 value corresponds to the slope of the straight part of experimental curve $f(t)=\ln([O_3]^0/[O_3]^t)$ measured at a long time (a_2), while, as expected, $\alpha\lambda_1+(1-\alpha)\lambda_2$ corresponds to the slope of the experimental curve measured at $t=0(a_1)$. Figure 5 shows the variation of α, λ_1, and λ_2 as a function of the photon flux at 11 K. A linear dependence of λ_2 with the photon flux is observed, whereas α and λ_1 appear independent of the photon flux. Figure 6 displays the logarithm of λ_1 and λ_2 vs reciprocal temperature for a flux of 0.38×10^{17} photon $cm^{-2}\,s^{-1}$. Arrhenius curves are linear for λ_1 and λ_2 and the same slope is observed. A linear dependence of α with the temperature is found.

In some experiments, measurements of the intensity decrease of ozone v_3 absorption were performed both from the higher and the lower component of the v_3 ozone band. At 11 K, same decay kinetics were observed for both bands. However at 21 K as displayed in Fig. 7, the second slope of the kinetic curve obtained from the lower component (ozone in a double site) was slightly larger than the slope of the kinetic curve obtained from the higher component (ozone in a single site). Unfortunately measurements at higher temperature could not be made because the higher component broadens when temperature increases and apparently vanishes above 25 K indicating a strong coupling with the matrix.

In order to complete the experimental study, an experiment at 11 K was performed with very highly diluted ozone in argon (O_3/Ar= 1/20 000). The obtained kinetic curve was compared at the kinetic curve of a O_3/Ar= 1/4000 sample obtained in the same condition (same photon flux). The two curves were similar and characterized by the same slopes a_1 and a_2.

DISCUSSION

Several models can reproduce the kinetics described by Eq. (3). In particular the observed overall ozone photolysis process is compatible with a set of two reversible photodissociation/reformation processes in combination with an irreversible destruction of ozone. Indeed, the observed

TABLE I. a_1 and a_2 experimental values and values of λ_1 and λ_2 calculated from Eq. (3) by fitting the experimental kinetic data (Fig. 3) obtained at 11 K for different photon flux (photons $cm^{-2}\,s^{-1}$).

Photon flux	3.2×10^{16}	3.8×10^{16}	6.4×10^{16}	8.4×10^{16}	11.4×10^{16}	15.2×10^{16}
a_1 (s^{-1})	0.83×10^{-3}	0.92×10^{-3}	0.95×10^{-3}	1.5×10^{-3}	1.1×10^{-3}	2.1×10^{-3}
a_2 (s^{-1})	1.1×10^{-4}	1.5×10^{-4}	1.7×10^{-4}	2.6×10^{-4}	2.5×10^{-4}	3.7×10^{-4}
α	0.2	0.25	0.21	0.28	0.3	0.32
λ_1 (s^{-1})	3.3×10^{-3}	2.8×10^{-3}	3.5×10^{-3}	4×10^{-3}	3.3×10^{-3}	4.6×10^{-3}
$\lambda_2\approx a_2$ (s^{-1})	1.1×10^{-4}	1.5×10^{-4}	1.7×10^{-4}	2.8×10^{-4}	2.6×10^{-4}	3.8×10^{-4}
$\alpha\lambda_1+(1-\alpha)\lambda_2\approx a_1$ (s^{-1})	0.7×10^{-3}	0.82×10^{-3}	0.9×10^{-3}	1.3×10^{-3}	1.2×10^{-3}	1.8×10^{-3}

TABLE II. a_1 and a_2 experimental values and values of λ_1 and λ_2 calculated from Eq. (3) by fitting the experimental kinetic data (Fig. 4) obtained at different temperatures with a photon flux of $(3.8\pm0.5)\times10^{16}$ photon cm^{-2} s^{-1}.

Irradiation temperature	11 K	16 K	18.5 K	21 K	26 K
a_1 (s^{-1})	0.9×10^{-3}	1.6×10^{-3}	2.1×10^{-3}	3×10^{-3}	9×10^{-3}
a_2 (s^{-1})	1.5×10^{-4}	2.2×10^{-4}	4.6×10^{-4}	8×10^{-4}	19×10^{-4}
α	0.25	0.35	0.4	0.5	0.6
λ_1 (s^{-1})	2.8×10^{-3}	3.2×10^{-3}	4×10^{-3}	5.8×10^{-3}	16×10^{-3}
$\lambda_2\approx a_2$ (s^{-1})	1.5×10^{-4}	2.6×10^{-4}	4.8×10^{-4}	7×10^{-4}	20×10^{-4}
$\alpha\lambda_1+(1-\alpha)\lambda_2\approx a_1$ (s^{-1})	0.8×10^{-3}	1.3×10^{-3}	1.9×10^{-3}	3.3×10^{-3}	10×10^{-3}

slow decay of ozone is suggesting that $O(^1D)$ produced by direct ozone photodissociation is efficiently quenched by argon atoms in the production site and that the $O(^3P)$ atom recombines with molecular oxygen to reform ozone. However, this process is in competition with the cage exit of a fraction of excited atomic oxygen atoms produced by dissociating ozone molecules which have the right orientation with respect to the ''windows'' of the cage. Formation of traces of a complex between the ground state oxygen atom with the ozone molecule is the proof that some excited oxygen atoms move out the cage. This hypothesis is also supported by the formation of N_2O when the argon matrix contains traces of N_2 molecules.[22] The nondependence of the kinetic curves with the ozone monomer concentration excludes the possibility that collision between $O(^1D)$ and ozone molecules in nearest neighbors could produce an excited $[O^*\cdots O_3]$ complex which should relax through two distinct channels, one by dissipating its energy in the matrix phonon bath, the other by dissociating into two oxygen molecules. Furthermore, numerical solutions obtained from a such model is not consistent with our experimental results.

Consequently, photodissociation of ozone could be described by the schematic following model:

$$O_3 \underset{\leftarrow}{\overset{k_1(v)}{\underset{k_2}{\rightleftarrows}}} O, O_2 \xrightarrow{k_3} O+O_2, \tag{4}$$

where k_1 is the photolysis rate constant defined in Eq. (2), k_2 is the recombination rate of the (O, O_2) pairs after quenching of $O(^1D)$, and k_3 the rate constant of the oxygen atom cage exit. In this model, the ozone concentration remaining after each irradiation period $[O_3]^t$ cannot be experimentally measured. Indeed, when irradiation is stopped, the (O, O_2) pair inside the cage recombines with a short time compared to the infrared observation time and only the relative concentration of atomic oxygens which escape from the cage can be deduced from the ozone v_3 band intensity. At $t=\infty$, the concentration of oxygen atom outside the cage $[O]^\infty$ is equal to the concentration of the initial ozone $[O_3]^0$,

$$[O]^\infty=[O_3]^0. \tag{5}$$

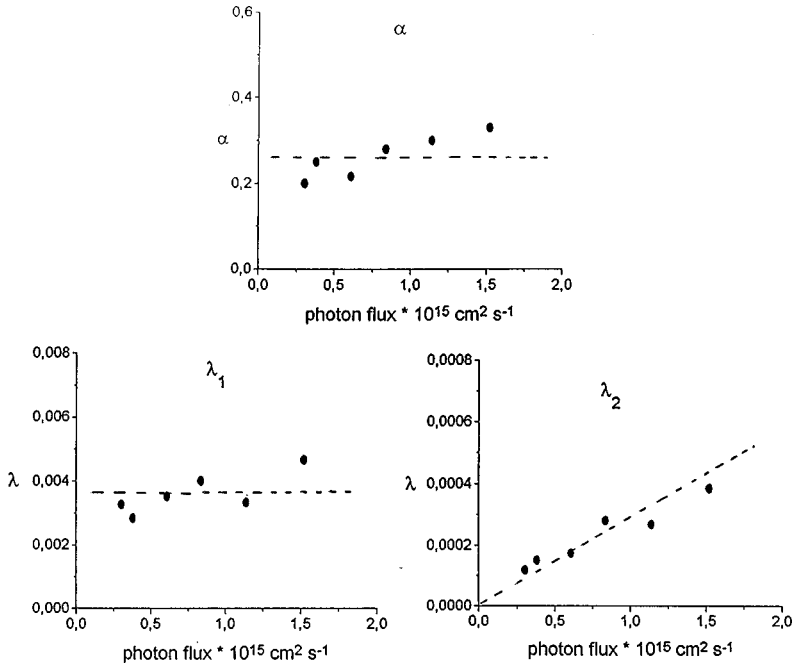

FIG. 5. Photon flux, (F) photons cm^{-2} s^{-1}; dependence for α, λ_1, and λ_2 parameters.

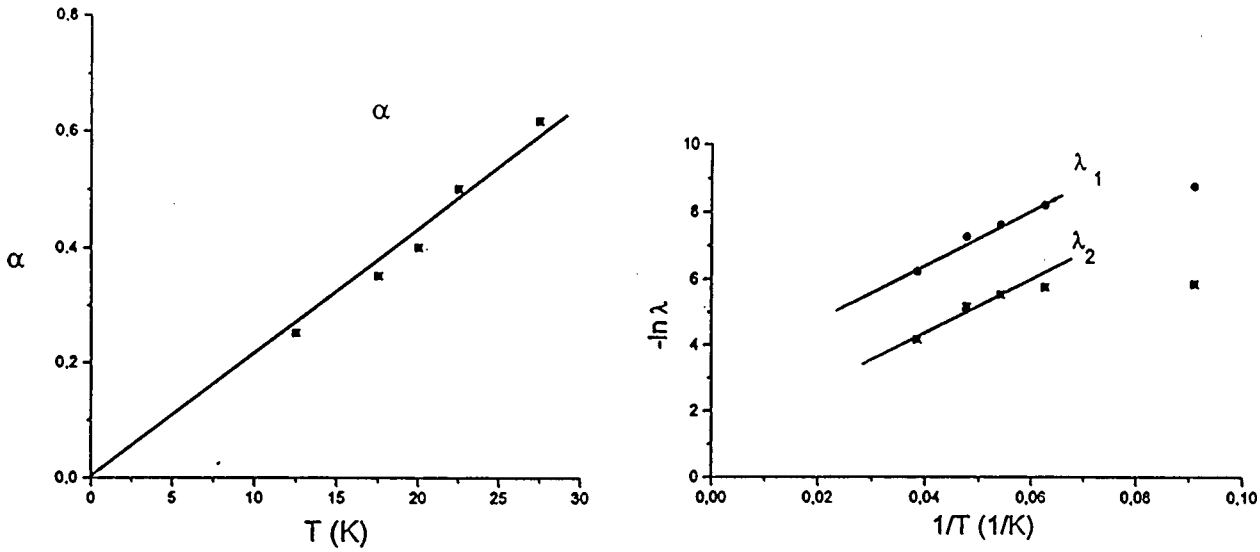

FIG. 6. Temperature dependence of α and Arrhenius plot of λ_1 and λ_2 parameters.

At time t, the concentration of oxygen atoms outside the original O_3 cages can be calculated from the initial concentration of ozone and from the concentration of ozone $[O_3^r]^t$ remaining at time t as follows:

$$[O]^t=[O_3]^0-[O_3^r]^t \text{ with } [O_3^r]^t=[O_3]^t+[O,\ O_2]^t. \tag{6}$$

Thus the curves of Figs. 2–4 represent the time evolution of the growth of oxygen atom after irradiation and not the dynamical decay of ozone during the irradiation. From the differential rate expressions describing reaction (4),

$$\frac{d[O_3]}{dt}=-k_1[O_3]+k_2[O,\ O_2], \tag{7}$$

$$\frac{d[O,\ O_2]}{dt}=k_1[O_3]-(k_2+k_3)[O,\ O_2], \tag{8}$$

$$\frac{d[O]}{dt}=k_3[O,\ O_2], \tag{9}$$

an analytical solution giving the concentration of oxygen atoms as a function of time can be obtained. It has the form

$$\ln\frac{[O]^\infty-[O]}{[O]^\infty}=\ln\frac{[O_3^r]^t}{[O_3]^0}$$
$$=\ln\left[\frac{k-\lambda_1-k_1}{\lambda_1-\lambda_2}e^{-\lambda_1 t}+\frac{k-\lambda_2-k_1}{\lambda_1-\lambda_2}e^{-\lambda_2 t}\right], \tag{10}$$

$$\lambda_1\lambda_2=k_1k_3,$$

$$\lambda_1+\lambda_2=k_1+k_2+k_3 \quad (\lambda_1>\lambda_2 \text{ is assumed}),$$

$$k=k_1+k_3.$$

As observed this solution can be fitted by Eq. (3), but the rate parameters λ_1 and λ_2 are not the elementary rate constants. Equations (3) and (10) are consistent for

$$\alpha=\frac{k-\lambda_1-k_1}{\lambda_1-\lambda_2}=\frac{k_3-\lambda_1}{\lambda_1-\lambda_2} \text{ or}$$

$$1-\alpha=\frac{k_3-\lambda_2}{\lambda_1-\lambda_2}=\frac{k-\lambda_2-k_1}{\lambda_1-\lambda_2}. \tag{11}$$

Variations of λ_1, λ_2, and α observed as functions of the photon flux and temperature are not understood easily with this model, however. The calculated value of $\lambda_1+\lambda_2$ is small with respect to the expected k_1 value. As an example, for $F=0.38\times10^{17}$ photon $cm^{-2}\,s^{-1}$ and assuming a quantum yield of 0.8 and a cross section $\sigma=8.5\times10^{-18}\,cm^2$ molecule^{-1} as in the gas phase, the estimated value of k_1 is 0.25 s^{-1}, a value of two orders of magnitude larger than the fitted value of $\lambda_1+\lambda_2$, i.e., $2.95\times10^{-3}\,s^{-1}$ (see values of λ_1 and λ_2 in Table I). Thus, during the irradiation period at 266 nm, it can be assumed that there is an equilibrium between the dissociation of O_3 with the formation of (O, O_2) pairs and either recombination of the pairs or

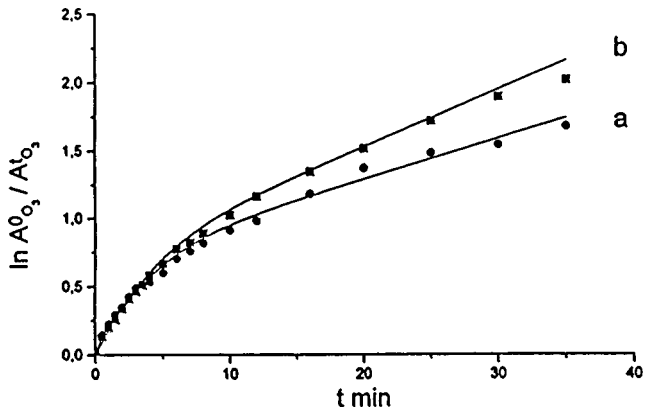

FIG. 7. Comparison of the kinetic curves for ozone decay at 21 K (a) in single site (●) and (b) in double site (■); O_3/Ar=1/4000; photon flux, 3.8×10^{16} photons $cm^{-2}\,s^{-1}$.

exit of atomic oxygen atoms leading to separate O and O_2 species. As a consequence the experimental kinetic curves describe the impulsive ejection of oxygen atoms into the lattice during the photodissociation of ozone, and not the primary ozone photodissociation process.

The distinct slopes observed in the plot of $f(t)$ could be explained by the existence of two classes of initial ozone molecules leading to different escape rates of oxygen atoms due to different spatial distributions of the reactant characteristic of fractal kinetics. Krueger and Weitz[27] studied the oxygen atom mobility in the xenon matrix and showed that the time dependence of the oxygen atom concentration was described by two bimolecular processes. A statistical theory for the sudden cage exit was presented by Zoval and Apkarian.[3] It was based on barrier height distribution due to the zero point energy and thermal fluctuations of the lattice, this distribution playing a key role in determining quantum yield of sudden cage exit.

The following scheme could then be considered to describe our experimental results:

$$[O_3,\ (O,\ O_2)]_a \xrightarrow{k_{3a}} O+O_2, \tag{12}$$

$$[O_3,\ (O,\ O_2)]_b \xrightarrow{k_{3b}} O+O_2, \tag{13}$$

leading to

$$[O_3^r]_a=\alpha[O_3]^0 e^{-k_{3a}t}, \tag{14}$$

$$[O_3^r]_b=(1-\alpha)[O_3]^0 e^{-k_{3b}t}, \tag{15}$$

and the atomic oxygen atom balance expression is

$$[O_3]^0=[O_3^r]_a+[O_3^r]_b+[O]^t, \tag{16}$$

where $[O]^t$ is the concentration of isolated (i.e., having left the initial cage where O_3 photodissociation occurred) oxygen atoms.

Combining these equation give

$$[O_3]^0-[O]^t=[O_3^r]^t=[O_3]^0[\alpha e^{-k_{3a}t}+(1-\alpha)e^{-k_{3b}t}], \tag{17}$$

from which k_{3a} and k_{3b} relate directly to the calculated λ_1 and λ_2 parameters and where α is the fraction of O_3 in the two classes a and b. If the exit rate for class a (i.e., $[O_3^r]_a$) is larger than that for class $b[O_3^r]_b$ the term $\alpha[O_3^0]\exp(-k_1t)$ becomes very small at a long time leading to a straight line for $f(t)$ with a slope of $-k_{3b}$ and an intercept at $t=0$ equal to $\ln[(1-\alpha)[O_3]^0$.

The observed variations of α, k_{3a}, and k_{3b} with the photon flux and with temperature show that (i) at 11 K a small fraction of O_3 ($\alpha=0.25$) has an orientation leading to a fast exit independent of the photon flux, whereas the major fraction of ozone leads to a slow oxygen exit which appears photo-induced; (ii) when temperature increases, the fraction of ozone which has the right orientation with respect to the windows of the cage increases and the two exit processes are faster than at 11 K. From the curves of Fig. 5, the same activation energy can be determined for the two processes and using an Arrhenius formula of the type $k_{obs}(T)=A\exp(-E_a/RT)$, a value of $E_a=0.5\pm0.1$ kJ mol^{-1} comparable of the value found in Ref. 20 was obtained.

CONCLUSION

Extensive studies of the photodissociation at 266 nm of the ozone monomer trapped in solid argon at 11 K have been undertaken at various photon fluxes and at different temperatures. Two distinct ozone decay rates which are temperature dependent were observed. The first one, the more rapid, occurs at a short time and is photon flux independent, whereas the second one observed at longer time is irradiation power dependent. Time dependence of the decrease of ozone is well fitted by a double exponential expression of the type

$$\ln\frac{[A]^t_{O_3}}{[A]^0_{O_3}}=\ln[\alpha\exp^{-\lambda_1 t}+(1-\alpha)\exp^{-\lambda_2 t}].$$

These observations are discussed and a model is proposed. The kinetic plots could correspond to two different cage escapes of a fraction of oxygen atoms produced by photodissociation of ozone in the cage, the exit rates depending on ozone orientations determined by temperature and excess energy of dissociation quantum yields. However, molecular dynamics simulations taking into account the experimental measurements should be useful for elucidating the overall mechanism of the photodissociation of ozone in an argon matrix.

ACKNOWLEDGMENT

The authors thank Dr. C. Camy-Peyret for reading the manuscript.

[1] J. Feld, H. Kunttu, and V. A. Apkarian, J. Chem. Phys. **93**, 1009 (1990).
[2] H. Bai and B. S. Ault, J. Phys. Chem. **96**, 9169 (1992).
[3] J. Zoual and V. A. Apkarian, J. Phys. Chem. **98**, 7945 (1994).
[4] F. Blatter and H. Frei, J. Phys. Chem. **97**, 1178 (1993).
[5] S. Laursen and G. C. Pimentel, J. Phys. Chem. **94**, 8175 (1990).
[6] A. de Saxce and L. Schriver-Mazzuoli, Chem. Phys. Lett. **199**, 596 (1992).
[7] *Chemistry and Physics of Matrix Isolated Species*, edited by L. Andrews and M. Moskovits (North–Holland, Amsterdam, 1989).
[8] M. E. Jacox and W. E. Thompson, J. Chem. Phys. **102**, 6 (1995).
[9] D. Forney and M. E. Jacox, J. Chem. Phys. **101**, 8290 (1994).
[10] J. N. Crowley and J. R. Sodeau, J. Phys. Chem. **93**, 4785 (1989); **93**, 3100 (1989).
[11] R. B. Bohn, G. D. Brabson, and L. Andrews, J. Phys. Chem. **96**, 1582 (1992).
[12] J. M. Parnis, L. E. Hoover, T. D. Fridgen, and R. D. Lafleur, J. Phys. Chem. **97**, 10708 (1993).
[13] J. A. Harrison and H. Frei, J. Phys. Chem. **98**, 12152 (1994).
[14] L. Schriver-Mazzuoli, B. Gauthier-Roy, D. Carrere, A. Schriver, and L. Abouaf-Marguin, Chem. Phys. **163**, 357 (1992).
[15] O. Abdelaoui, L. Schriver, and L. Schriver-Mazzuoli, J. Mol. Struct. **268**, 335 (1992).
[16] L. Schriver-Mazzuoli, O. Abdelaoui, and A. Schriver, J. Phys. Chem. **96**, 8069 (1992).
[17] C. Lugez, A. Schriver, R. Levant, and L. Schriver-Mazzuoli, Chem. Phys. **181**, 129 (1994).
[18] M. V. Pettersen, A. Schriver, L. Schriver-Mazzuoli, P. Chaquin, and E. Lasson, Chem. Phys. **204**, 115 (1996).
[19] L. Schriver-Mazzuoli, A. Schriver, and Y. Hannachi, J. Phys. Chem A **102**, 10221 (1998).
[20] A. V. Benderskii and C. A. Wight, J. Chem. Phys. **101**, 292 (1994).
[21] A. V. Benderskii and C. A. Wight, Chem. Phys. **189**, 307 (1994).

[22] M. Bahou, L. Schriver-Mazzuoli, C. Camy-Peyret, and A. Schriver, J. Chem. Phys. **108**, 6884 (1998).
[23] H. A. Michelsen, R. J. Salawitch, P. O. Wenberg, and J. G. Anderson, Geophys. Res. Lett. **21**, 2227 (1994).
[24] L. Schriver-Mazzuoli, A. Schriver, C. Lugez, A. Perrin, C. Camy-Peyret, and J. M. Flaud, J. Mol. Spectrosc. **176**, 85 (1996).
[25] P. Brosset, R. Dahoo, B. Gauthier-Roy, L. Abouaf-Marguin, and A. Lakhlifi, Chem. Phys. **172**, 315 (1993).
[26] L. Schriver-Mazzuoli, A. de Saxce, C. Lugez, C. Camy-Peyret, and A. Schriver, J. Chem. Phys. **102**, 690 (1995).
[27] H. Kruger and E. Weitz, J. Chem. Phys. **96**, 2846 (1992).